Activity-dependent model of axonal targeting in the developing olfactory bulb driven by population coded chemosensor input

Daljeet S. Gill[a], Keith J. Albert[b], David R. Walt[b,*], and Tim C. Pearce[a,*]

[a]Department of Engineering, University of Leicester, Leicester LE1 7RH, United Kingdom *Corresponding author for computational work. Tele: +44(0)116.223.1290 Fax: +44(0)116.252.2619; Email: t.c.pearce@leicester.ac.uk

[b]The Max Tishler Laboratory for Organic Chemistry, Department of Chemistry, Tufts University, Medford, MA 02155 *Corresponding author for sensor work. Fax: 617.627.3443; Email: david.walt@tufts.edu

Abstract

Two recent studies revealed that odorant-evoked activity-dependent competition is significant in the organisation and maintenance of the olfactory system. In this paper, we investigate the generation of a chemotopic sensory map in the olfactory bulb through three models driven by high-density optical chemosensor arrays which have similar properties to olfactory receptor neurons. By exposing the sensor arrays to various odours and Hebbian learning these models achieve self-organisation, potentially explaining the activity-dependent competition demonstrated by recent experimental studies. Our final model also predicts a role for periglomerular cells in the formation of the chemotopic sensory map.

Introduction

Activity-dependent mechanisms are known to play a pivotal role in the development of ocular dominance columns (ODCs) in the visual system[1-3]. The formation of ODCs is perhaps the most widely studied phenomenon in neural development due to the profound influence of neural activity on their development. The seminal work of Hubel and Wiesel on monocular deprivation[4] has led to numerous modelling studies conducted to better understand the development of ODCs[5]. Von der Malsburg and Willshaw were amongst the first to implement models of ODCs based on activity[6,7].

The early olfactory pathway has emerged as a significant model for studying axonal plasticity due to its continual turnover of olfactory receptor neurons (ORNs)[8]. This pathway is unique in the Central Nervous System (CNS) in that it must continually replenish stocks of ORNs in order to maintain the sense of smell, since the lifespan of ORNs is between a few weeks to months[9]. The precise targeting of ORNs onto the first synaptic target, known as glomeruli (schematised in Figure 1a), is therefore crucial in the developing olfactory bulb (OB). A key issue remains how this targeting takes place and the role of activity dependent mechanisms in this process, which is the subject of this paper.

In the olfactory system, evidence is now emerging that activity-dependent mechanisms similar to those seen in the formation of ODCs in the visual system, such as competition between axons for survival and space, are responsible for the generation of a chemotopic sensory map in the OB. In particular, two recent studies have shown that odorant-evoked activity influences the organisation and maintenance of the OB[16,17]. Zheng et al. genetically induced competition by breeding triple mutant mice in which half of the M72 (a specific OR gene) expressing ORN population is active and the other half inactive by selectively knocking out the cyclic nucleotide-gated (CNG) channel[16]. Their results show that active and inactive ORNs segregate to individual glomeruli rather than intermingling, suggesting that odorant-evoked competition exists between active and inactive M72 ORN types which directs their final targeting (Figure 1b). More recently Zhao and Reed demonstrated that ORNs without the CNG channel are slowly and specifically depleted from the olfactory epithelium (OE) and OB while functional ORNs are retained[17] (Figure 1c). This implies that odorant-evoked activity is crucial for neuronal survival and plays a role in the organisation and maintenance of the early olfactory pathway.

The central question addressed in this paper is the potential for activity-dependent plasticity mechanisms to explain these recent experimental observations in glomerular targeting. We investigate the formation of topographic projections due to odorant-evoked activity only. We use high-density optical chemo sensor arrays which have similar properties to ORNs in terms of specificity of response, number of independent responses and transient responses, in order to drive our models with realistic input[18-23].

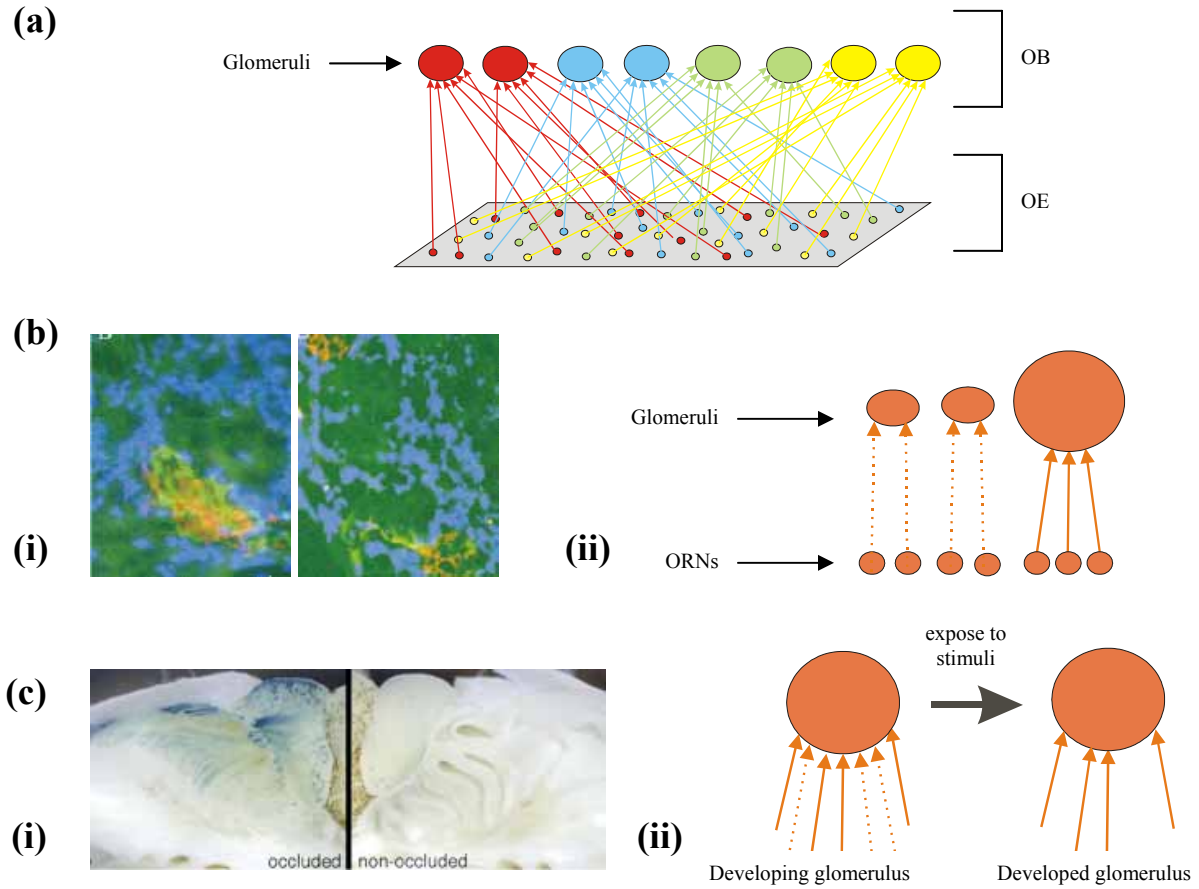

Figure 1 (a) A schematic diagram showing axonal targeting in a developed early olfactory pathway. A particular olfactory receptor neuron (ORN) within the olfactory epithelium (OE) is likely to express only one of the ~1000 odorant receptor (OR) genes (in mice) encoded in the mammalian genome[10,11]. ORNs expressing a given OR gene (each gene shown as a specific colour) project their axons and converge with extraordinary accuracy onto two or a few neighbouring glomeruli[12-14] (among the ~1800 glomeruli[15]) in the olfactory bulb (OB). For clarity only four ORN types with two glomeruli each are shown. (b)(i) The left diagram shows a double fluorescence imaging technique used to visualise the projections of 2 different ORN populations (in green and red colour) expressing the same OR gene co-converging onto the same glomeruli (dense innervation bottom centre of picture) in the OB when their cyclic nucleotide-gated (CNG) channels were functioning. The right diagram shows segregation between active and inactive ORNs (top left and bottom right) supposedly due to competition. Axons without functional CNG channels (in red colour) project to separate and smaller glomeruli. (Reproduced from Zheng et al. (2000)[16]).(ii) A schematic diagram showing ORNs expressing the same OR gene segregate to distinct glomeruli depending on functioning and non-functioning CNG channels. ORNs without functional CNG channels converge onto separate and smaller glomeruli instead of intermingling with axons of neurons with functional CNG channels. (c)(i) Figures showing the path taken by axons of ORNs form OE to OB. The left diagram shows both active and inactive ORNs (axons of ORNs are blue in colour) survive and converge onto their respective glomeruli (can be seen by the extensive innervation of blue axons) when odour stimulation was blocked. The right diagram shows a depletion of inactive ORNs (i.e. axons in blue colour no longer exist. Compare to figure on its left.) when odorants were allowed to enter the nasal cavity (Reproduced from Zhao and Reed (2001)[17]).(ii) A schematic diagram showing how inactive ORNs innervating a single glomerulus are depleted (when the system is exposed to odorants during development) due to activity-dependent competition between ORNs with and without functioning CNG channels. (For both (b)(ii) and (c)(ii) the dotted lines refer to axons of ORNs without a functional CNG channel. ORNs with functional CNG channels are indicated by solid lines.)

Experimental

We describe three models that account for the experimental observations outlined in Figure 1 and detailed in references 16 and 17. For the first two models (Figure 2a), the sensor responses to odour "Air" were used to mimic spontaneous neural activity to achieve inactive ORNs (odour deprived).

In the first experiment (a single glomerulus shown in Figure 2a), identical sensor beads (representing the ORN population of a single type) with identical broad tunings to a set of odorants (see [18-23] for experimental details on sensor bead technology and imaging apparatus) were used to demonstrate the survival of the active, and depletion of inactive, ORNs as observed by Zhao and Reed[17]. Half of the sensor bead population was deprived of odour stimuli while a repeating sequence of odours were applied to the remaining half. 500 sensors were exposed to odour "Air" and the remaining 577 sensors to various odours (in the following order: acetone, benzene, chloroform, Colombian coffee, cyclohexanone, 1,3-dinitrobenzene, 2,4-dinitrotoluene, ethanol, n-propanol, heptane, methanol, toluene, and water). The odour "Air" and a selected odour (from the total 13 odours) were exposed simultaneously to the sensors. All of the weighted inputs from individual sensor beads (representing a total of 1077 ORNs) innervate a single glomerulus. The 1077 ORNs were assigned weights $w_{ij}(t) = (i = 1, 2, 3, ..., 1077)$ to target G_j generating output y_j which were subjected to Hebbian learning. Hebbian learning increases the weights in proportion to the product of postsynaptic activity $y_j(t)$ and input activity $x_i(t)$. Subtractive normalisation imposes a constraint on Hebbian learning by subtracting the averaged weight value (averaged across all synapses impinging onto a single target i.e. glomerulus) from each weight value to stabilise the Hebbian plasticity rule, Eq. (1). If the weight value of a synapse is greater than the averaged weight value, it will increase towards the upper limit (usually set to 1). And if the weight value is less than the averaged weight value, the weight will decrease towards its lower limit (usually set to 0). Eventually, the weights of synapses w_{i1} that converge to the upper limit are deemed to survive while those that converge to the lower limit are considered depleted from the system. This normalisation constraint was used to enforce competition within the model and takes the form[24]

$$\frac{dw_{i1}}{dt} = y_1 x_i - \frac{y_1(\mathbf{n}.\mathbf{x}^T)}{N_x}, \qquad (1)$$

where $\mathbf{n}.\mathbf{x}^T$ is the sum of all inputs and $\mathbf{n}$ is a N_x dimensional vector (N_x =1077) with all its elements equal to 1. For the first model, j =1 as only a single glomerulus was considered. All weight values were initially randomised between 0 and 1.

Next, a similar experiment was conducted to demonstrate the segregation of weights for active and inactive ORN populations for different glomeruli observed by Zheng et al.[16]. Here, the number of glomeruli was increased to 4 to permit segregation of inputs. Initially, all weights were randomly uniformly distributed in the range 0,1. Oja's rule, a local learning rule, was used to show the separation between the active and inactive ORN populations[25]. By restricting the length of each weight vector (column j of w_{ij}), competition between the different weights is imposed since an increase in one weight forces other weights to decrease. Such an arrangement is compatible with one population of ORNs having an advantage for acquiring neurotrophic factors through electrical activity allowing an increase in uptake of these factors. This rule forces the weight decay to be proportional to the output squared, y_j^2. By multiplying each synaptic strength w_{ij} with y_j^2 (for the jth glomerulus) the length of each weight vector is fixed following a phase of Hebbian learning. The synaptic weight vector is normalised according to the following equation

$$\frac{dw_{ij}}{dt} = \alpha(y_j x_i - y_j^2 w_{ij}), \qquad (2)$$

where α is the learning rate.

The schematic diagram for our final experiment is shown in Figure 2b. A randomised array of 2 sensor bead types is employed and was exposed to all the fourteen odours (including air). The purpose of our final

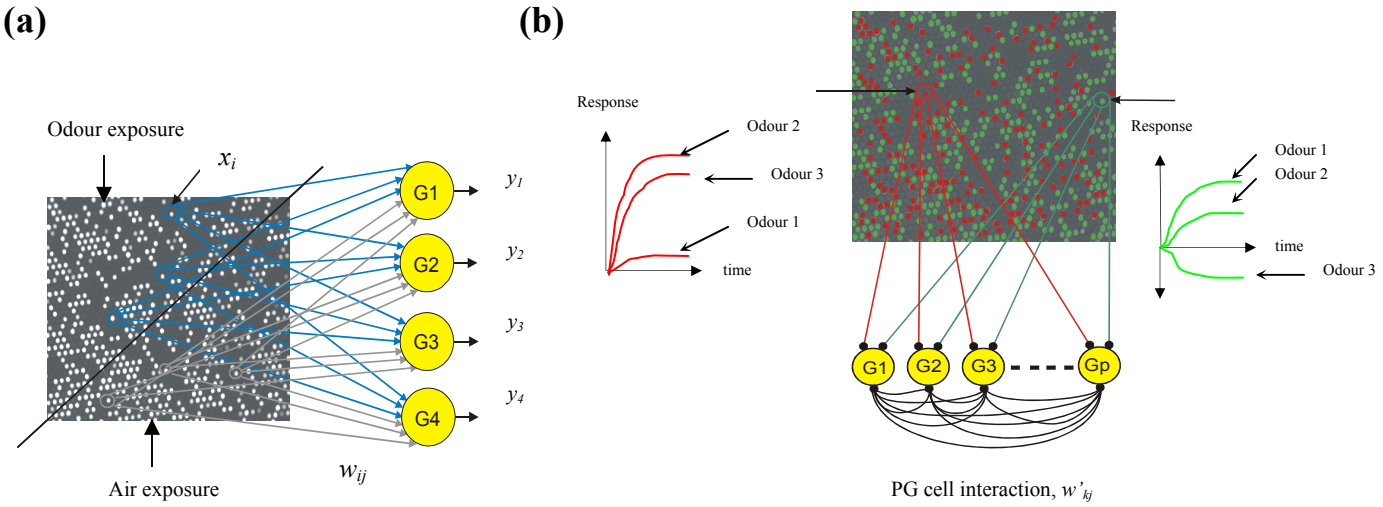

Figure 2 Schematic diagram for the 3 experiments. The first 2 experiments are shown in (a) and the final experiment in (b). All the sensors mimic ORNs. Approximately half the total sensors in (a) and all sensors in (b) were exposed to various odours (note: the remaining sensors in (a) were exposed to odour "Air" only) and the sensor response values (x_i - shown in (a) is a single value for an individual sensor) were extracted. The extracted sensor response profiles formed the realistic input data to the models and the weights, w_{ij}, of all ORNs were subjected to Hebbian learning to achieve self-organisation. Each sensor's diameter is 3μm. (a) A population of identical sensors has half its population exposed to odour "Air" only (representing inactive ORNs and all their weights are shown in grey colour) and the other half to various odours (representing active ORNs with weights in blue colour) (separated by a diagonal solid line), each connected by a weight, w_{ij} (note: w_{i1} for the first experiment in (a) since there is only one glomerulus), to an individual glomerulus G1 (in yellow colour). Only 1 glomerulus (G1) with output (y_1) was used in the first experiment to demonstrate first depletion of inactive ORNs. The second experiment used the same set-up as the first but all 4 glomeruli (G1-G4) are employed to achieve segregation between the 2 populations of the same type. (b) 2 sensor types (red and green colour) representing 2 receptor gene types consisting of 587 sensors randomly distributed on an optical array platform, similar to the distribution of ORNs in OE, are used to show segregation in weight values between different sensor types and the effect of periglomeruli (PG) cells via lateral connections on the formation of a structured glomerular map. Each sensor type gives a unique response to a set of odour stimuli. The response of each sensor in the array is bipolar (i.e. positive or negative). Lateral connections between all the glomeruli (G1 to Gp) models possible interglomerular interactions within the bulb.

experiment was to test the potential role of perglomeruli (PG) cells in organising local topological structure in the OB glomeruli. An arbitrary choice of 21 glomeruli were deployed with lateral connections representing PG cells interactions in the OB. We represent the effect of PG cells through lateral connections (shown in Figure 2b). The following equation was used to achieve this effect,

$$y_j = \sum_i w_{ij} x_i + \sum_{k \neq j} w'_{kj}\, y_k \quad , \qquad (3)$$

where y_j is the total activity of the jth glomerulus in the model. The synaptic weights connecting the kth glomerulus to jth glomerulus are represented by w'_{kj} (termed recurrent weights). The first term on RHS of Eq. (3) corresponds to the activation due to the feedforward input while the second term represents the combined effect of all the lateral connections. As in the case of the first two experiments, all initial weight values were randomised between 0 and 1. The recurrent weights w'_{kj} were assigned according to the Mexican Hat function (depicted in Figure 3c (top)) and are fixed. The Mexican Hat function encourage nearby cell activity to be correlated, and they therefore adapt to similar stimuli (local excitatory connections) while distant cells (larger distance inhibitory connections) perform the opposite task by fostering anticorrelated activity hence preventing adaptation to input stimuli. This function, which allows the model to concentrate its electrical activity into local clusters, takes the form

$$w'_{kj} = \left(Ae^{-(k-j)^2/\sigma_1^2}\right) - \left(Be^{-(k-j)^2/\sigma_2^2}\right), \quad (4)$$

where the term *k-j* refers to the position of *k*th glomerulus from *j*th glomerulus. *A* and *B* are constants set to 5 and 4 respectively to ensure the peak amplitude of the Mexican Hat function equals to 1. The standard deviations σ_1^2 and σ_2^2 control the width of the Mexican Hat function and were set to 3.87 and 5.48 respectively. By including recurrent connections we investigate whether a topologically structured map arises that is compatible with the known topology of the glomerular map in the OB. Oja's rule (Eq. 2) was used here together with the Mexican Hat function (Eq. 4) to achieve both separation of the two input populations and organisation of the glomeruli in the OB in view of the lack of detailed anatomical data in the biology.

Results

In the first experiment, 2 separate weight clusters formed corresponding to weighted connections to odour deprived and odour exposed populations, indicating the odour deprived population was systematically depleted from the glomerulus whilst the other survived due to activity dependent competition between inactive and active ORNs (Figure 3a). The results resemble those observed in the experiment conducted in by Zhao and Reed[17]. A 98.79% correct connection scheme (in terms of the number of active ORNs that were expected to survive) was achieved across the entire population. Figure 3a shows the number of active ORNs reduce to 564 from 577. Of the 13 active ORNs that failed to establish correct connections, 11 had their weight values reduced to zero (depleted) increasing the number of inactive ORNs to 511. These errors are likely to be due to deviant sensor beads that became malformed during fabrication. All the deviant sensor beads could have been removed from the input data beforehand by performing statistical analysis to test for outliers (as shown in our previous studies- refer to references 18 and 23). However, the input data used in this paper were not pre-screened in order for it to be applied to the models in its raw form. The reason for this is we wanted to test the models under realistic noisy conditions and therefore did not selectively adjust the data set.

In the second experiment we show separation between the 2 input populations (active and inactive) across the 4 glomeruli, indicating that sensors segregate to different glomeruli and do not intermingle, despite being of the same type (Figure 3b). Each glomerulus (G1 to G4) has 2 clusters of synaptic weight values which shows segregation between active and inactive ORNs. The cluster with higher weight values corresponds to the ORN population that emerged as the victor in the odorant-evoked competition. All clusters with large weight values in Figure 3b represent the ORN populations responsible for driving their respective glomerulus activity. In our model, G1 and G4 activities are largely driven by active ORNs while G2 and G3 activities are largely driven by inactive ORNs. Despite generating 2 clusters with distinct weight values, each glomerulus gave only a 98.42% correct segregation between active and inactive inputs. This is due to the overlap in weight values between a few deviant sensor beads that exist in the different sensor populations. Over repeated experiments no topographical order to glomeruli tuning was demonstrated. This experiment illustrates how activity dependent mechanisms can potentially assist organisation of the developing OB in terms of establishing segregation of glomeruli with distinct stimuli tunings.

The results from the final experiment show glomeruli organising themselves into a topologically structured map depending on the type of ORNs they are innervated by as a result of introducing PG cell mediated lateral connectivity (Figure 3c). Without lateral connections the previous model generates random patterns of selectivity across the glomerular layer since no activity dependent competition was initiated between neighbouring glomeruli. The PG cell interaction enables inter-glomerular interactions within the OB by introducing short-range excitatory and long-range inhibitory lateral connections (Figure 3c (top)) between the 21 glomeruli. The glomeruli are seen to be activated in clusters due to this lateral connectivity scheme (Figure 3c). The clustered glomeruli activity patterns lead to competition between different groups of glomeruli allowing glomeruli dominant for either the green or red sensor types (see Figure 2b and 3c) to be organised in a pattern of alternating stripes. Specifically, Glomeruli 10-15, and 21-4 formed two stripes for green sensor type while the remaining glomeruli formed stripes for the red sensor type indicating clustering of glomeruli of the same tuning (note that in our model glomeruli 1 and 21 are "neighbours"). Our results suggest that PG

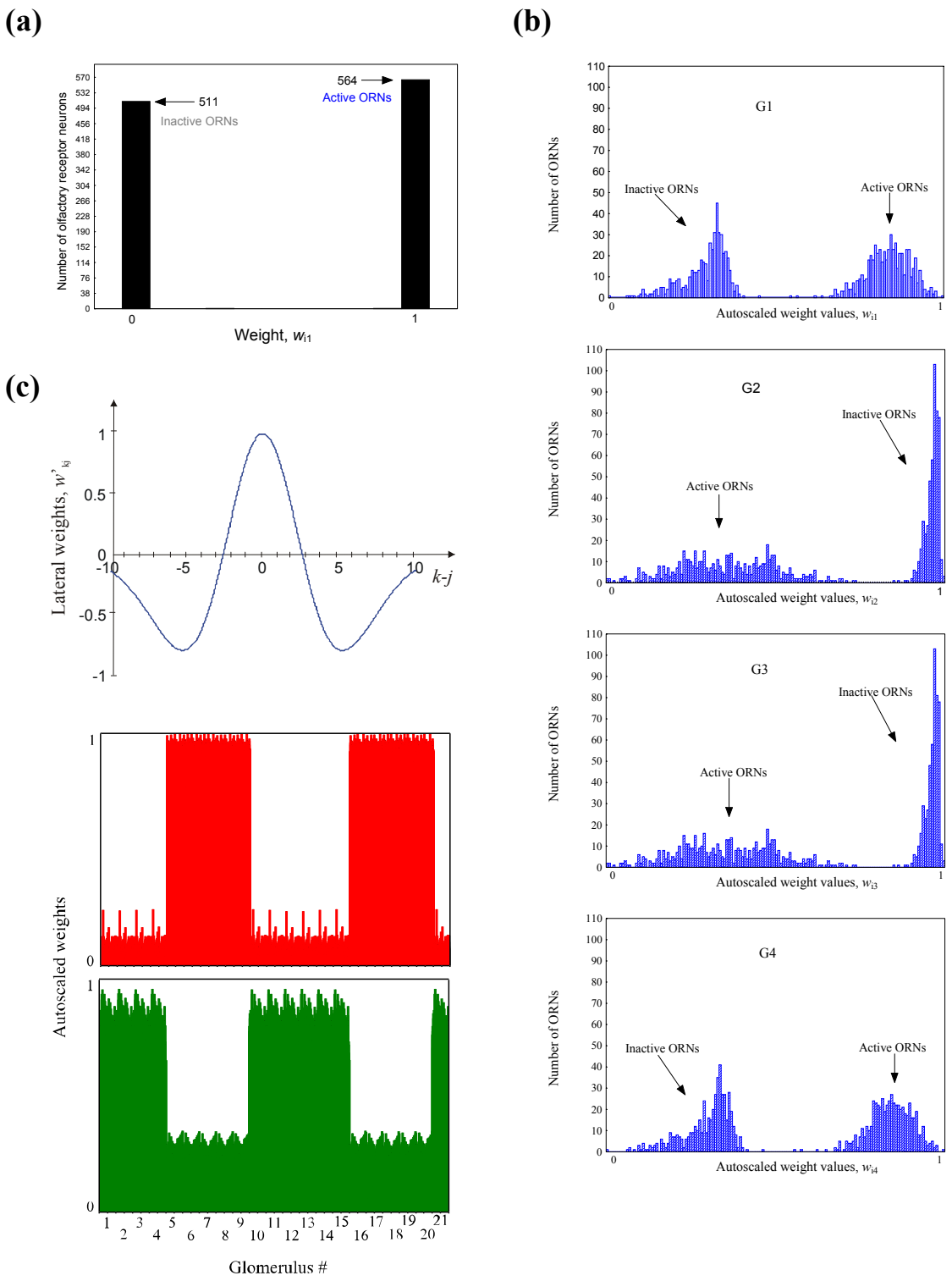

Figure 3 (a) Plot showing 2 clusters of weight values which largely separate the inactive (weight value 0) and active ORNs (weight value 1) for a single glomerulus. A total of 13 deviant beads were located of which 11 had their weight values equal to zero. (b) The innervation of ORNs to each of the 4 glomeruli (G1 to G4) is dominated (in terms of larger synaptic weight values) by one population of ORNs (either active or inactive) due to competition between the inputs. Each plot shows 2 clusters (corresponding largely to ORN populations) of weight values where the cluster with higher weight values emerge as victors in the competition to drive the glomeruli activity. Of the 4 glomeruli, 2 (G1 and G4) were innervated by active ORNs and the other 2 (G2 and G3) by inactive ORNs. However, over repeated experiments (with randomised initial weight values) no order to the tunings emerged. (C) Plots showing the organisation of glomeruli weights after evolution with lateral connectivity. By applying the lateral connectivity function (top) a structured

glomerular layer was formed. The lower plots show 2 sensor types (green type and red type as mention in Figure 2b) each innervating a group of glomeruli in close proximity. Only 200 sensors from each type were plotted for clarity purposes (total 400 out of 587 sensors). A total of 21 glomeruli were used where glomeruli 10-15, and 21-4 were innervated by the green ORNs and the rest by red ORNs. Note: glomeruli 1 and 21 are "neighbours".

cells may play a role in the organisation of glomeruli belonging to specific OR gene expressing ORNs by mediating activity dependent competition between neighbouring glomeruli.

The model presented in this experiment demonstrates a potential role for PG cells in the organisation of the glomeruli in the OB. The competition between the 2 randomly distributed sensor types resulted in a 100% correct segregation based on their characteristic response to various odours. This shows that by exposing the randomised array (which has different ORN types distributed randomly across its surface reminiscent of the OE) to various odours, self-organisation can be achieved to explain the convergence and competition process.

Discussion and conclusion

Three separate experiments were conducted to explain the recent experimental observations in the developing OB based on odorant-evoked activity-dependent competition. By employing two different optical sensor platforms used for artificial chemical sensing applications, we investigated the generation of a chemotopic sensory map in the OB driven by realistic input. These platforms were exposed to odours and Hebbian learning was used to achieve self-organisation. For the first model we showed that inactive ORNs are systematically depleted from the olfactory system as a result of being deprived of odorant exposure, indicating that odorants and the activity they evoke are potentially significant in the developing olfactory system. Next, we demonstrated competition between 2 populations of ORNs expressing the same OR gene through the segregation of active and inactive ORN populations. As shown in Figure 1b(ii) in the case of the biology active and inactive ORNs do not converge onto a single glomerulus but instead segregate to individual glomeruli. Here an allele is deprived of activity by knocking out the olfactory cyclic nucleotide-gated channel (OCNC) gene which codes for an ion channel in the olfactory signal transduction pathway. This experiment was termed "monoallelic deprivation" by Zheng et al. (2000)[16] since one allele was deprived of activity but not the other. This and other experiments demonstrate parallels in the activity-dependent mechanisms in the visual system, originally uncovered by Wiesel and Hubel[4] with the developing olfactory system.

The final model implements competition between 2 different populations of ORNs and gives rise to a prediction regarding the role of PG cells in organising OB topology. The model predicts that PG cells may potentially contribute to the organisation of the glomeruli in the OB. In the biology, PG cells provide interactions between glomeruli, and may receive input directly from ORNs. These cells make reciprocal dendrodendritic contacts with mitral and tufted cells. It is therefore possible that these PG cells could contribute to grouping similar types of glomeruli since they mediate between glomeruli, ORNs, and mitral and tufted cells. Though the glomeruli are not connected to each other directly in the OB, we claim that PG cells may play a parallel role as the lateral interactions between cortical neurons in the visual system. The results in Figure 3c show grouping of glomeruli over many cell units, similar to the formation of ODCs. The number of cells within a cluster of glomeruli is a function of the form and scaling of Eq. (4) and the only purpose of presenting our results in this way is to show clear clustering of same type glomeruli. However, it is important to note that ORNs expressing the same OR generally converge in the biology onto two or a few specific glomeruli in the OB.

In all the three models, only the role of activity-dependent competition of axonal targeting in the developing OB has been investigated, no role for chemical guidance cues is considered. It is important to note that in the biology only some specific OR expressing ORNs (e.g. M72) may be influenced by activity while others (e.g. P2) are not affected at all by odorant-evoked neuronal activity. This difference may be due to M72 glomerulus forming later than P2 glomerulus (which develops prenatally in mice) and therefore experience-dependent plasticity may be important. For all ORNs, chemical guidance cues play a prominent role prior to the OB stage. The different axon targeting stages involved prior to the OB are not discussed in this paper.

We showed that activity-dependent competition may be crucial to the organisation and maintenance of the olfactory system. Three models driven by high-density optical chemosensor arrays which have similar properties to ORNs were used to investigate the generation of a chemotopic sensory map in the OB. We also provide a prediction for the role of PG cells in the formation of this chemotopic sensory map. We compare our models closely to the formation of ODCs which perhaps offer the best characterised activity-dependent competition model in neural development. This is the first time activity-dependent mechanisms are investigated in the developing olfactory system using realistic data through modelling and can provide a framework for future studies on the role of PG cells in OB topographic organisation.

Acknowledgements
The Leicester work is funded by the European Commission (to TCP), the Engineering and Physical Science Council (to TCP), and the Royal Society, London (to TCP) and the Tufts work is supported by the Defense Advanced Research Projects Agency and Department of Energy (to DRW).

REFERENCES

[1] Crowley, J.C. and Katz, L.C., *Current Opinion in Neurobiology,* 2002. **12:** 104-109
[2] Katz, L.C. and Shatz, C.J., *Science,* 1996. **274:** 1133-1138
[3] Stryker, M.P., *Neurosci. Res. Prog. Bull.,* 1982. **20:** 540-549
[4] Wiesel, T.N. and Hubel, D.H., *J. Neurophysiol*.,1963. **26:** 1003-1017
[5] Swindale, N.V., *Network: Computation in Neural Systems*, 1996. **7:** 161-247
[6] Von der Malsburg, Ch. and Willshaw, D.J., *Exp. Brain Res.*, 1976. **1:** 463-469
[7] Willshaw, D.J. and Von der Malsburg, Ch., *Proc. R. Soc. B*, 1976. **194:** 431-445
[8] Graziadei, P.P.C. and Monti-Graziadei, G.A., *J. Neurocytol*., 1979. **8:** 1-18
[9] Mombaerts,P., *Nature Neuroscience*, 2001. **4:** 1192-1198
[10] Buck, L.B., *Annu. Rev. Neurosci.*, 1996. **19:** 517-544
[11] Malnic, B., Hirono, J., Sato, T. and Buck, L.B., *Cell*, 1999. **96:** 713-723
[12] Ressler K.J., Sullivan S.L. and Buck, L.B., *Cell*, 1994. **79:** 1245-1255
[13] Vassar, R., Chao, S.K., Sitcheran, R., Nunez, J.M., Vosshall, L.B. and Axel, R., *Cell*, 1994. **79:** 981-991
[14] Mombaerts, P., Wang, F., Dulac, C., Chao, S.K., Nemes, A. Mendelsohn, M., Edmondson, J. and Axel, R., *Cell*, 1996. **87:** 675-686
[15] Royet, J.P., Souchier, C., Jourdan, F. and Ploye, H., *J. Comp. Neurol.*, 1988. **270:** 559-568
[16] Zheng, C., Feinstein, P., Bozza, T., Rodriguez, I. and Mombaerts, P., *Neuron*, 2000. **26:** 81-91
[17] Zhao, H. and Reed, R.R., *Cell*, 2001. **104:** 651-660
[18] Albert, K. J., Gill, D. S., Pearce, T. C. and Walt, D. R., *Analytical Chemistry*, 2001. **73:** 2501-2508
[19] Albert, K. J. and Walt, D. R., *Analytical Chemistry*, 2000. **72:** 1947-1955
[20] Dickinson, T. A., Michael, K. M., Kauer, J. S. and Walt, D. R., *Analytical Chemistry,*1999. **71:** 2192-2198
[21] Albert, K. J., Lewis, N. S., Schauer, C. L., Sotzing, G. A., Stitzel, S. E., Vaid, T. P. and Walt, D. R., *Chem. Rev.*, 2000. **100:** 2595-2626
[22] Stitzel, S. E., Cowen, L., Albert, K. J. and Walt, D. R., *Analytical Chemistry*, 2001. **73:** 5266-5271
[23] Albert K.J., Gill D.S., Pearce T.C. and Walt D.R., *Analytical and Bioanalytical Chemistry,* 2002, **373:** 792 to 802
[24] Dayan, P. and Abbott, L., Theoretical Neuroscience: Computational and mathematical modelling of neural systems, 2001. MIT Press, Cambridge.
[25] Wyatt, J.L. and Elfadel, I.M., *Neural Computation*, 1995. **7:** 915-922